

Supporting Information

Cobalt Single-Atom Catalysts with High Stability for Selective Dehydrogenation of Formic Acid

*Xiang Li, Annette-Enrica Surkus, Jabor Rabeah, Muhammad Anwar, Sarim Dastgir, Henrik Junge, Angelika Brückner, and Matthias Beller**

anie_202004125_sm_miscellaneous_information.pdf

Supporting Information

Table of Contents

1. General Experimental Details	2
2. Calculation of gas production rate.....	4
3. Preparation of Co-N-C Heterogeneous Catalyst	5
3.1 Synthesis of ZnCo-BMOF.....	5
3.2 Synthesis of Co-ZIF-67	5
3.3 Synthesis of Zn-ZIF-8	5
3.4 Synthesis of Co-N-C(SACs) catalyst	5
3.5 Synthesis of Co-N-C(NPs) catalyst.....	6
3.6 Synthesis of Co(1)/phen(7)/C catalyst.....	6
4. Comparison of Heterogeneous Catalysts for the Dehydrogenation of FA.....	7
5. Procedure for the Dehydrogenation of FA	8
5.1 Burette measurements	8
5.2 Procedure for the dehydrogenation of FA	8
5.3 GC spectra.....	11
6. Characterization of the Cobalt Catalyst.....	13
6.1 Elemental Analysis	13
6.2 XRD Measurements	13
6.3 N₂ Adsorption Measurements	14
6.4 XPS results of catalysts	15
7. Test on the Stability of Active Sites for Co-N-C (SACs) and Co-N-C (NPs).....	16
8. Long-term Experiments.....	18
9. Fitting Results of EXAFS.....	20
10. TEM	21
11. NMR	22
12. Mechanistic Proposal for Formic Acid Dehydrogenation	23
References	24

1. General Experimental Details

Dehydrogenation reactions were performed under Ar with exclusion of air using standard Schlenk techniques. Formic acid (FA) was purified by reflux and distilled following standard procedures and then stored under argon atmosphere. Water was degassed by bubbling argon for 8 hours. Solvents were used directly without purification. HCO_2Na and LiBF_4 were used and stored as received. The metal precursors $\text{Co}(\text{NO})_3 \cdot 6\text{H}_2\text{O}$, $\text{Zn}(\text{NO})_3 \cdot 6\text{H}_2\text{O}$ and KOH were obtained from Alfa Aesar, 2-methylimidazole were obtained from Arcos Organics chemicals, all these reagents were used directly without further purification.

The power X-ray diffraction (PXRD) pattern was carried out on a Stoe STADI P diffractometer, equipped with a linear Position Sensitive Detector (PSD) by $\text{Cu K}\alpha$ radiation ($\lambda = 1.5406 \text{ \AA}$). The software WinXpow (Stoe) was used for processing. The patterns were assigned according to the Powder Diffraction File (PDF) database of the International Centre of Diffraction Data (ICDD).

EPR (electron paramagnetic resonance) spectra were recorded on an X-band Bruker EMX CW-micro EPR spectrometer equipped with an ER4119HS high-sensitivity resonator using a microwave power of Ca 6.9 mW, modulation frequency of 100 kHz and modulation amplitude up to 5 G. For low temperature measurements, the EPR spectrometer was equipped with a temperature controller and liquid N_2 cryostat. For Ph_3P ligand involved test, EPR spectrum of Co-SACs (6 mg) was firstly measured at 100 K then excess amount of Ph_3P (10 mg) was added to the EPR tube, heated to 90 °C (just above the melting point of Ph_3P (80 °C)), and measured again the EPR spectrum at 100 K.

TEM (Transmission Electron Microscopy) measurements were performed on a Thermo Fisher Titan Themis, 60-300 “cubed” microscope fitted with an aberration-correctors for the imaging and the probe forming lens at 300 kV. The microscope was also equipped with an energy-dispersive x-ray-spectrometer (EDXS) for chemical analysis. For pretreatment, powder was dispersed in isopropyl alcohol and sonicated for about 10 minutes. Then a 20 μL of the dispersed solution was dropped over 300 mesh Cu grid and dried at room temperature for TEM analysis

The X-ray absorption spectra were collected on the beamline BL01C1 in NSRRC. The radiation was monochromatized by a Si (111) double-crystal monochromator. XANES and EXAFS data reduction and analysis were processed by Athena software. The obtained XAFS data was processed in Athena

(version 0.9.25) for background, pre-edge line and post-edge line calibrations. Then Fourier transformed fitting was carried out in Artemis (version 0.9.25). The k^2 weighting, k -range of 3 - 12 \AA^{-1} and R range of 1 - ~ 3 \AA were used for the fitting. The model of bulk Co, CoPc and Co_3O_4 were used to calculate the simulated scattering paths. The four parameters, coordination number, bond length, Debye-Waller factor and E_0 shift (CN, R , σ^2 , ΔE_0) were fitted without anyone was fixed, constrained, or correlated. For Wavelet Transform analysis, the $\chi(k)$ exported from Athena was imported into the Hama Fortran code. The parameters were listed as follow: R range, 1 - 4 \AA , k range, 0 - 13 \AA^{-1} ; k weight, 2; and Morlet function with $\kappa=10$, $\sigma=1$ was used as the mother wavelet to provide the overall distribution.

The XPS (X-ray Photoelectron Spectroscopy) measurements were recorded with a VG ESCALAB220iXL with monochromated $\text{AlK}\alpha$ radiation ($E = 1486.6$ eV). All curves were deconvoluted with Gaussian-Lorentzian curves for quantitative analysis. Meantime, the peak areas were divided by a sensitivity factor from the element specific Scofield factor and the transmission function of the spectrometer.

N_2 adsorption isothermal curves were tested by the instrument of ASAP 2020 from Micromeritics (USA). Measurements were done with standard BET procedure:

- a): pretreatment of the sample up to 400 $^\circ\text{C}$ at 0.01 mbar to desorb gases and water
- b): adsorption and desorption of N_2 at -196 K with a low pressure from 3×10^{-6} (P/P_0)
- c): calculations: BET-plot, t -plot and pore size distribution via DFT (model: slit pores for carbon)

Gas content was determined by gas-phase GC (6890A, Agilent Technologies). The gas was analyzed by two detection systems:

GC a): HP Plot Q / FID – hydrocarbons, Carboxen / TCD - permanent gases, He carrier gas.

GC b): Carboxen / TCD / Methanizer / FID - permanent gases, He carrier gas.

The H_2 , CO_2 , CO , and CH_4 amounts were determined and their ratios established.

2. Calculation of gas production rate

The gas production rate was calculated by equation (S1):

$$\text{Gas production rate} = \frac{V_{gas}}{m_{cat} \times t} \quad (\text{S1})$$

where V_{gas} is the gas volume corrected by blank volume, and m_{cat} is the weight of catalyst, respectively.

The turnover frequency (TOF) was calculated by equation (S2):

$$TOF = \frac{\frac{V_{gas}}{(V_{m,H_2,25^\circ C} + V_{m,CO_2,25^\circ C})}}{n_{cat} \times t} \quad (\text{S2})$$

The calculation of $V_{m,H_2,25^\circ C}$ and $V_{m,CO_2,25^\circ C}$ were carried out using equation (S3) and (S4):

$$V_{m,H_2,25^\circ C} = \frac{RT}{p} + b - \frac{a}{RT} = 24.48 \frac{L}{mol} \quad (\text{S3})$$

$$V_{m,CO_2,25^\circ C} = \frac{RT}{p} + b - \frac{a}{RT} = 24.36 \frac{L}{mol} \quad (\text{S4})$$

Where:

R: $8.3145 \text{ m}^3 \cdot \text{Pa} \cdot \text{mol}^{-1} \cdot \text{K}^{-1}$;

T: 298.15 K;

P: 101325 Pa;

a (H₂): $24.7 \cdot 10^{-3} \cdot \text{Pa} \cdot \text{m}^6 \cdot \text{mol}^{-2}$ and a (CO₂): $36.5 \cdot 10^{-2} \cdot \text{Pa} \cdot \text{m}^6 \cdot \text{mol}^{-2}$;

b (H₂): $26.6 \cdot 10^{-6} \text{ m}^3 \cdot \text{mol}^{-1}$ and b (CO₂): $42.7 \cdot 10^{-6} \text{ m}^3 \cdot \text{mol}^{-1}$

3. Preparation of Co-N-C Heterogeneous Catalyst

3.1 Synthesis of ZnCo-BMOF

The synthesis method was referenced by Wang et al. Typically, $\text{Co}(\text{NO}_3)_2 \cdot 6\text{H}_2\text{O}$ (0.546 g) and $\text{Zn}(\text{NO}_3)_2 \cdot 6\text{H}_2\text{O}$ (1.116 g) were mixed and dissolved in 30 mL of methanol as solution 1. Then, 2-methylimidazole (1.232 g) was dropped into a 30 mL of methanol as solution 2. The solution 1 was subsequently added to solution 2 under vigorously stirring for 6 hours at room temperature. As-obtained precipitates were collected by centrifugation at 5000 rpm for 20 minutes, washed five times with methanol, and finally dried overnight.

3.2 Synthesis of Co-ZIF-67

The procedure was same as the synthesis of ZnCo-BMOF except for $\text{Zn}(\text{NO}_3)_2 \cdot 6\text{H}_2\text{O}$ introduction. Typically, $\text{Co}(\text{NO}_3)_2 \cdot 6\text{H}_2\text{O}$ (0.546 g) was dissolved in 30 mL of methanol as solution 1. Then, 2-methylimidazole (1.232 g) was dropped into 30 mL of methanol as solution 2. The solution 1 was subsequently added to solution 2 under vigorously stirring for 6 hours at room temperature. As-obtained precipitates were collected by centrifugation at 5000 rpm for 20 minutes, washed five times with methanol, and finally dried overnight.

3.3 Synthesis of Zn-ZIF-8

The procedure was the same as ZnCo-BMOF synthesis except for $\text{Co}(\text{NO}_3)_2 \cdot 6\text{H}_2\text{O}$ introduction. Typically, $\text{Zn}(\text{NO}_3)_2 \cdot 6\text{H}_2\text{O}$ (1.116 g) was dissolved in 30 mL of methanol as solution 1. Then, 2-methylimidazole (1.232 g) was dropped into a 30 mL of methanol as solution 2. The solution 1 was subsequently added to solution 2 under vigorously stirring for 6 hours at room temperature. As-obtained precipitates were collected by centrifugation at 5000 rpm for 20 minutes, washed five times with methanol, and finally dried overnight.

3.4 Synthesis of Co-N-C(SACs) catalyst

The dried powder of ZnCo-BMOF was calcinated with a heating rate of $10\text{ }^{\circ}\text{C min}^{-1}$ kept at $800\text{ }^{\circ}\text{C}$ for 1 hour, $900\text{ }^{\circ}\text{C}$ for 1 hour and $1000\text{ }^{\circ}\text{C}$ for 1 hour under argon flow in a tube furnace. Then it naturally cooled to room temperature. As-prepared samples were directly used without acid etching and other post-treatment. Notably, the catalysts which labelled with Co-SACs-X, meaning X was the final calcination temperature. For Co-SACs-800 and Co-SACs-900, the final temperatures were kept at $800\text{ }^{\circ}\text{C}$ and $900\text{ }^{\circ}\text{C}$ for 3 hours, respectively.

3.5 Synthesis of Co-N-C(NPs) catalyst

The dried powder of Co-ZIF-67 was calcinated with a heating rate of $10\text{ }^{\circ}\text{C min}^{-1}$ kept at $800\text{ }^{\circ}\text{C}$ for 1 hour, $900\text{ }^{\circ}\text{C}$ for 1 hour and $1000\text{ }^{\circ}\text{C}$ for 1 hour under argon flow in a tube furnace. Then it naturally cooled to room temperature. As-prepared samples were directly used without acid etching and other post-treatment. Notably, the catalysts which labelled with Co-NPs-X, meaning X was the final calcination temperature. For Co-NPs-800 and Co-NPs-900, the final temperatures were kept at $800\text{ }^{\circ}\text{C}$ and $900\text{ }^{\circ}\text{C}$ for 3 hours, respectively.

3.6 Synthesis of Co(1)/phen(7)/C catalyst

The synthesis method was same like provided in our previous report. Typically, $\text{Co(OAc)}_2\cdot 4\text{H}_2\text{O}$ (126.8 mg, 0.5 mmol) and 1,10-phenanthroline (3.5mmol) (Co:phenanthroline = 1:7 molar ratio) were stirred in ethanol (20 mL) for 30 minutes at room temperature. Then Vulcan XC72R carbon (696 mg) was added and the mixture was stirred at $60\text{ }^{\circ}\text{C}$ for 4 hours with refluxing. The ethanol was removed by a rotary evaporator and dried overnight. The black powder was grinded and transferred into a ceramic crucible for calcination in the oven. The oven was heated to $800\text{ }^{\circ}\text{C}$ at a rate of $25\text{ }^{\circ}\text{C per min}$ and held at $800\text{ }^{\circ}\text{C}$ for 2 h under argon, then cooled to room temperature.

4. Comparison of Heterogeneous Catalysts for the Dehydrogenation of FA

Table S1. Heterogeneous catalysts for the dehydrogenation of FA.

Catalyst	Other reactants	Temp. [°C]	TOF [h ⁻¹]	Ref.
Mono-metallic system				
Pd/C	citric acid/ Sodium formate	25	64	[1]
Pd/N-C _M (≈2.6 nm)	No	100	436	[2]
Pd/NH ₂ -MIL-125	Sodium formate	32	214	[3]
Au clusters/Al ₂ O ₃	Triethylamine	25	64	[4]
Au clusters/ZrO ₂	Triethylamine	25	252	[5]
Pd/C _m	Sodium formate	60	7256	[6]
Pd@CN900K	Sodium formate	60	14400	[7]
Bimetallic system				
AgPd alloy NPs (≈4 nm)	No	50	230	[8]
AgPd alloy NPs (≈2.2 nm)	No	50	382	[9]
AgPd/MIL-101	Sodium formate	80	848	[10]
PdAu/C-CeO ₂	Sodium formate	92	227	[11]
Ag ₁₈ Pd ₈₂ @ZIF-8	Sodium formate	80	580	[12]
AuPd/NH ₂ -N-rGO (≈2.2 nm)	Sodium formate	40	7953	[13]
Trimetallic system				
Pd _{0.58} Ni _{0.18} Ag _{0.24} /C(≈5.6 nm)	Sodium formate	50	85	[14]
Au _{0.28} Pd _{0.47} Co _{0.25} /MIL-101-NH ₂	No	25	347	[15]
PdAuEu/C	Sodium formate	92	387	[16]
Co _{0.30} Au _{0.35} Pd _{0.35} /C	No	25	80 ^a	[17]
CoAuPd/DNA-rGO	No	25	85 ^a	[18]
Ni _{0.40} Au _{0.15} Pd _{0.45} /C	No	25	12 ^a	[19]
Only non-noble metal				
Co(1)/phen(7)/C	No	98	220 ^a	[20]
Co-N-C (SACs)	No	98	357 ^a	This work

^aInitial TOF values calculated for the initial stages of the catalytic reactions.

5. Procedure for the Dehydrogenation of FA

5.1 Burette measurements

As shown in figure S1, the setup of activity measurements was done by a 3-neck double wall reactor attached to a condenser and manual burettes.

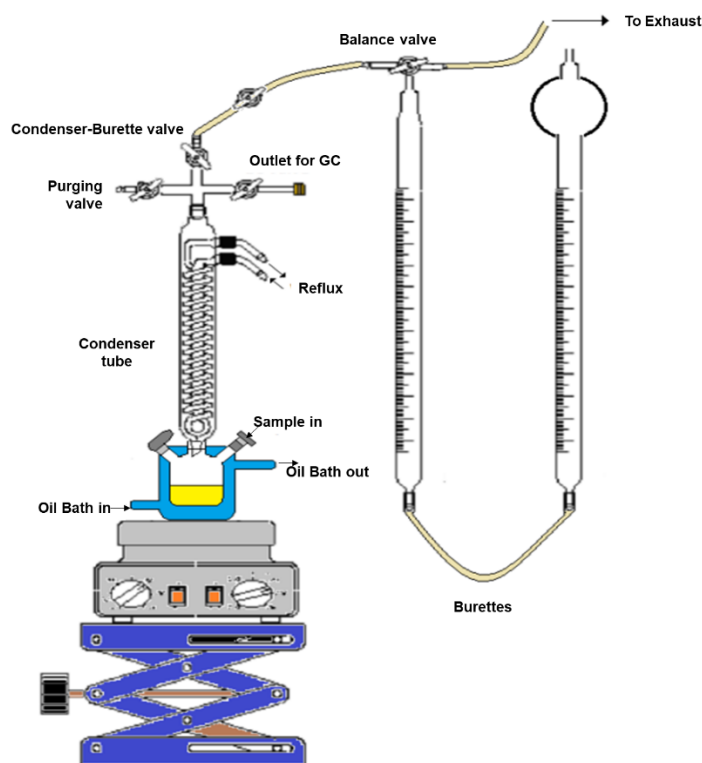


Figure S1. Manual burette setup.

5.2 Procedure for the dehydrogenation of FA

The reaction vessel was evacuated and flushed with argon 6 times. FA (10 mmol, 377 μ L) and solvent were added under an argon flow. The vessel was heated to the desired temperature with the help of thermostate and let equilibrate for 20 min. Then, the catalyst (30 mg) was dropped into the reaction vessel under argon flow with a mini-Teflon cup. Then the setup was vented to the open air to release the pressure in the burette, closed again, followed by starting measurement of the evolved gas volume using a manual burette. After finishing the reaction during the desired time, the degassed syringe was used to obtain a gas sample analyzed by gas chromatography.

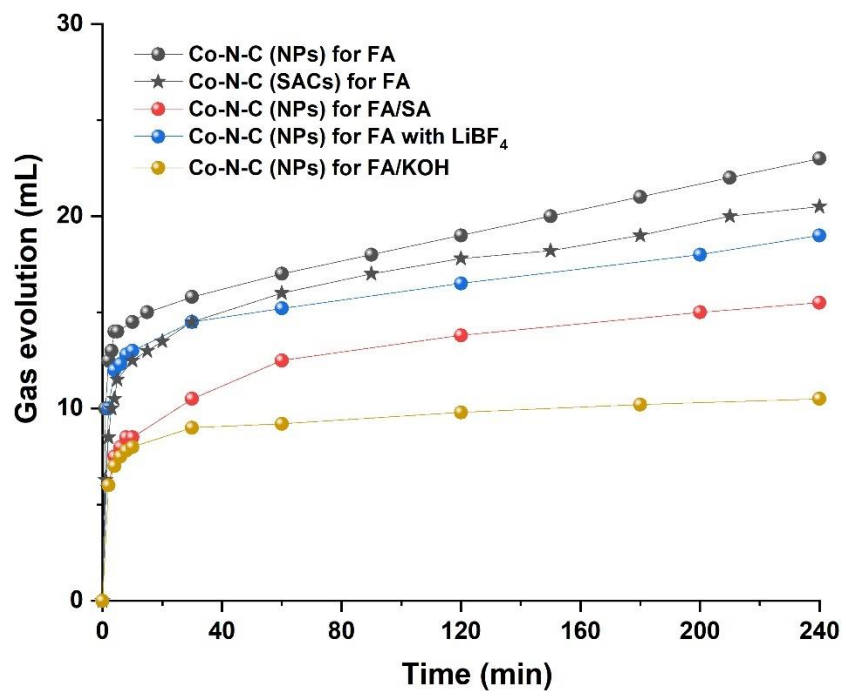


Figure S2. Investigation of pH and additive effect on the Co-N-C catalysts. Reaction conditions: FA (10 mmol) or FA (1.35 mmol) with SA (8.65 mmol) for pH of 7 or FA (10 mmol) with KOH (15 mmol) for pH of 14, catalyst (30 mg) in water (6 mL). Furthermore, LiBF₄ doping with 1mmol when used.

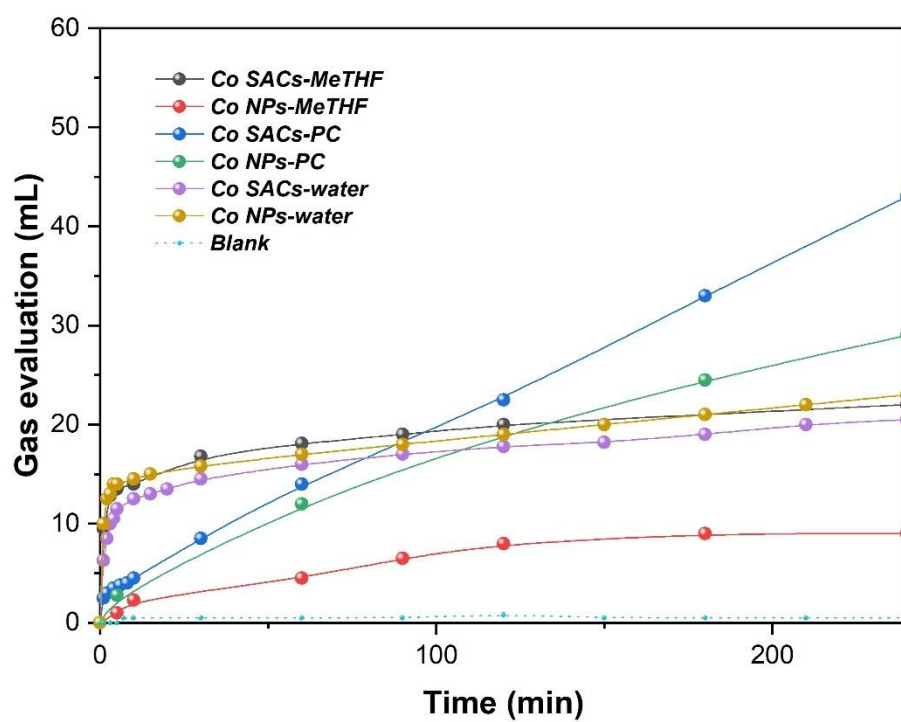


Figure S3. Investigation of the effect of solvent using on gas evaluation. Reaction conditions: FA (10 mmol) and catalyst (30 mg) in solvent (6 mL).

5.3 GC spectra

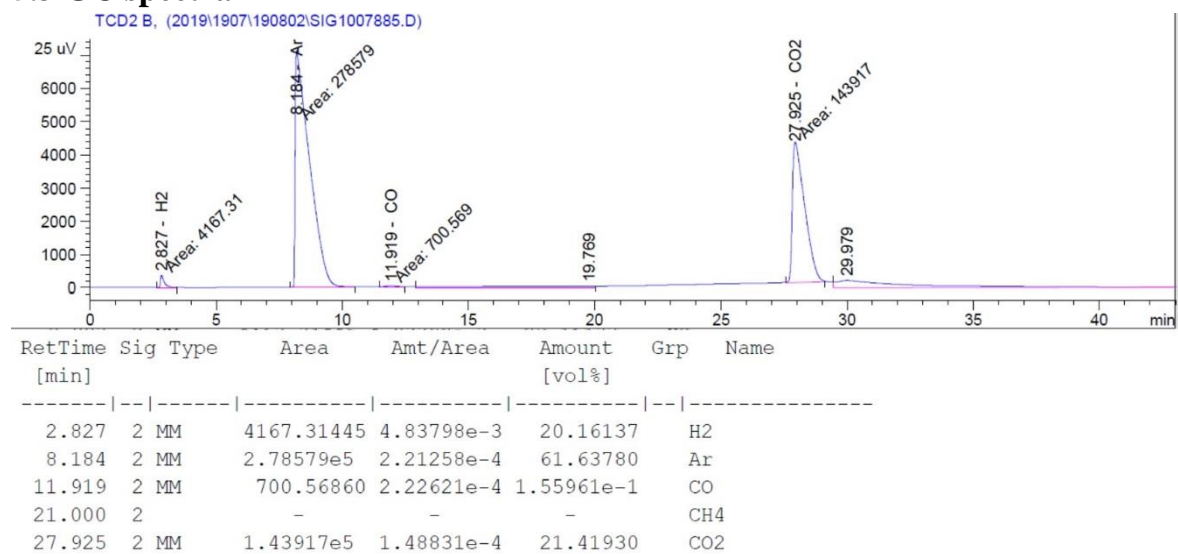


Figure S4. GC spectra. Reaction conditions: HCOOH (10 mmol, 377 μ L), Co-SACs (30 mg) in PC (6 mL), T_{set} : 110 $^{\circ}$ C, T_{actual} : 98 $^{\circ}$ C, 20 h.

Table S3. CO content and H₂ : CO₂ ratios for the DH of FA^a.

Experiment	V _{H₂+CO₂} ^b (mL)	H ₂ Vol% ^c	CO ₂ Vol% ^c	CO ^c (Vol%)	Vol%H ₂ /(Vol% CO ₂)	Time (h)
Co-N-C(SACs)/PC-110°C	140	48.3	51.3	0.37	0.94	20
Co-N-C(NPs)/PC-110°C	100	47.9	52	0.12	0.92	20
Co-N-C(SACs)/H ₂ O-100°C	52	40.1	59.9	0.06	0.67	20
Co-N-C(NPs)/H ₂ O-100°C	50	32.1	66.9	1.01	0.48	20
Co-N-C(SACs)/MeTHF-85°C	22	n.d.	99.8	0.22	-	4
Co-N-C(NPs)/MeTHF-85°C	10	28	71.8	0.2	0.39	4
Co-N-C(NPs)/H ₂ O-100°C, neutral ^d	16	74.7	25	0.33	2.99	4
Co-N-C(NPs)/H ₂ O-100°C, Base ^e	12	94.4	5.6	n.d.	16.9	4
Co-N-C(NPs)/H ₂ O-100°C, LiBF ₄ ^f	19	58.8	41.1	0.11	1.43	4

^aReaction conditions detailed under the corresponding table/experiment in this work. ^bGas evolution monitored with manual burettes. ^cContent of the gas phase analyzed by GC with a CO detection limit of 10ppm, n.d. stands for “not detected”. ^dHCOONa is doped with a molar ratio to HCOOH is 32 to 5 to get a neutral condition with pH of 7. ^eKOH is doped with a molar ratio to HCOOH is 2 to 3 to get a base condition with pH of 14. ^fLiBF₄ is doped as additives with a 10% molar ratio.

6. Characterization of the Cobalt Catalyst

6.1 Elemental Analysis

Table S4. Elemental Analysis

Catalyst	EA (wt%)		
	Co	N	Co:N (molar ratio)
Co-N-C(SACs)-1000	1.355	6.619	0.2
Co-N-C(NPs)-800	39.36	2.033	19.4

6.2 XRD Measurements

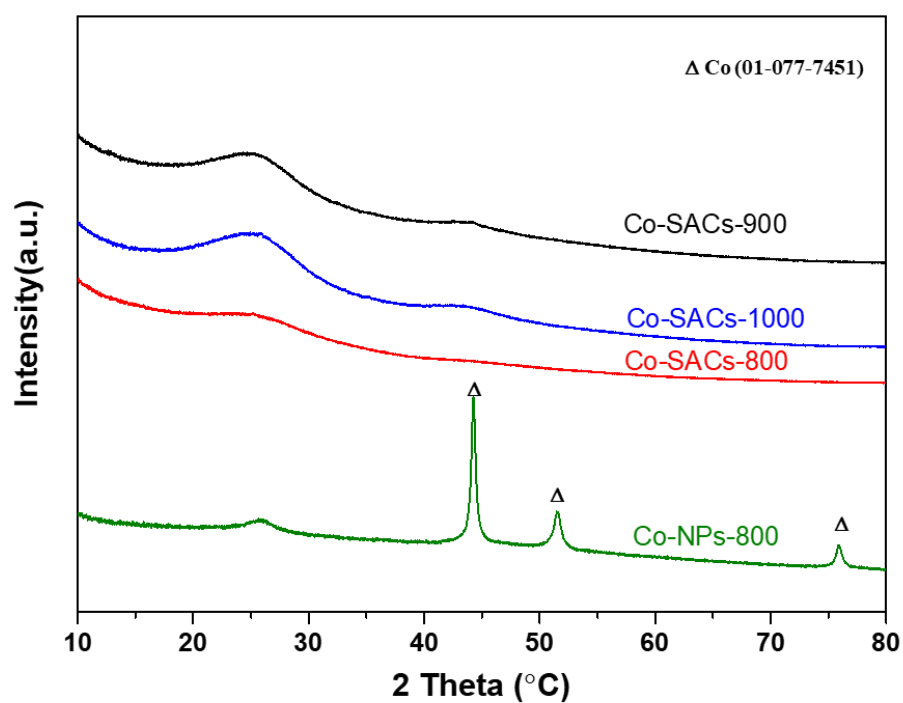


Figure S5. XRD spectra of the catalysts.

6.3 N₂ Adsorption Measurements

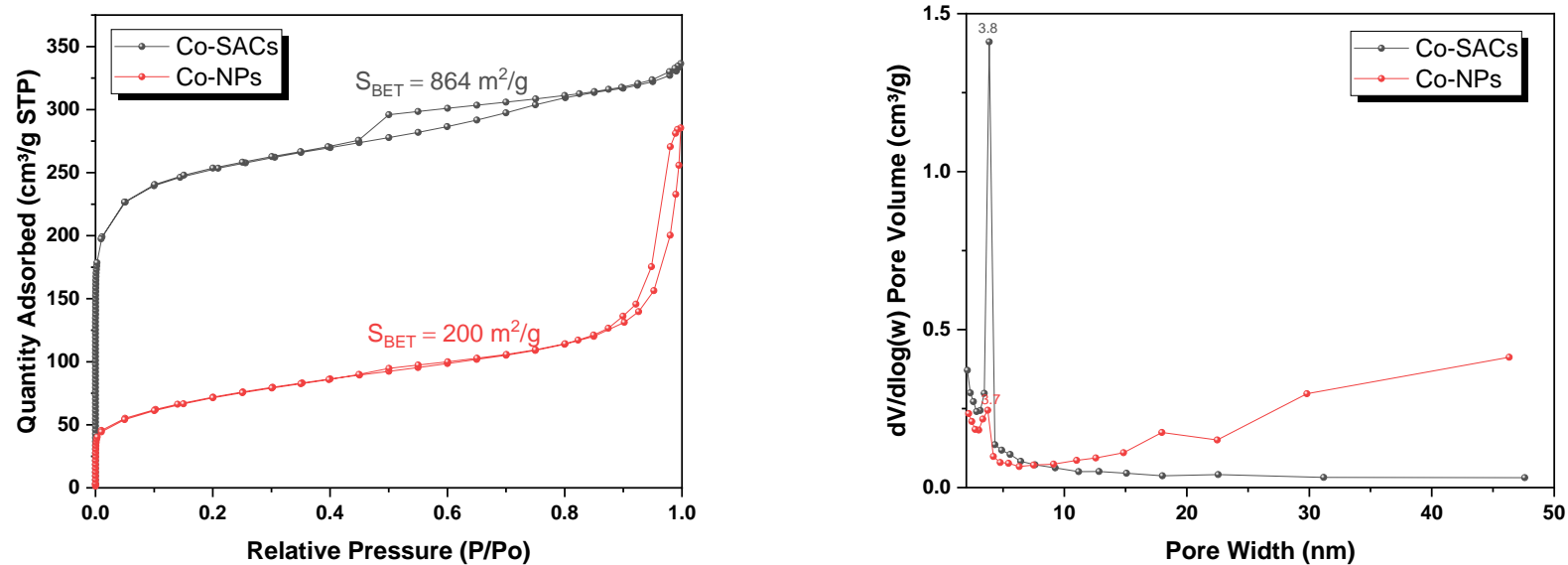


Figure S6. N₂ Adsorption isotherm (left) and pore size distribution (right) of the catalysts.

Co-N-C (SACs) catalyst has a quadruple BET surface area but similar pore size (~3.7 nm) to Co-N-C (NPs).

6.4 XPS results of catalysts

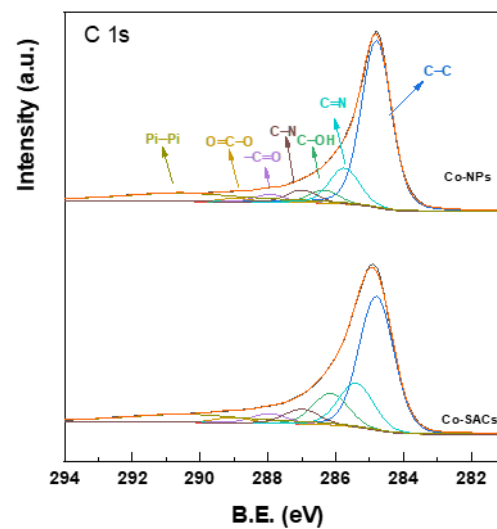


Figure S7. C1s xps curves of samples

Table S5. Surface concentration results by XPS

Catalyst	C-C (at%)	C=N (at%)	C-N (at%)	CO (at%)	OCO (at%)	Pi-Pi (at%)	C-OH (at%)	Total C (at%)	Pyridinic (at%)	Pyrrolic (at%)	Graphitic (at%)	N-O (at%)	Total N (at%)	Co (at%)
Co-N-C (SACs)	41.14	13.53	4.52	2.93	1.58	10.88	9.77	84.35	4.87	2.22	0.37	-	7.46	0.38
Co-N-C (NPs)	51.79	11.18	3.89	2.37	1.13	13.24	4.02	87.62	3.71	1.51	0.18	-	5.4	2.25

7. Test on the Stability of Active Sites for Co-N-C (SACs) and Co-N-C (NPs)

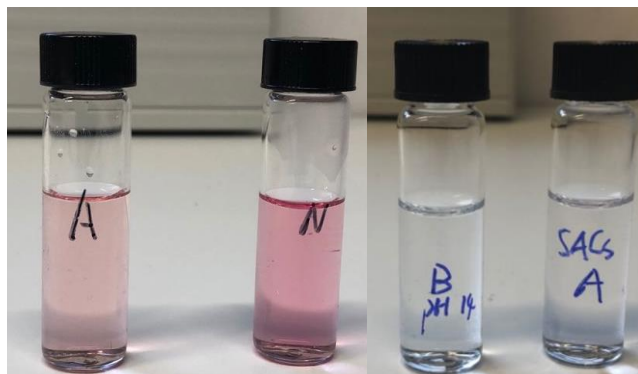


Figure S8. Colour change phenomenon of solvent after reaction (water as solvent): A for acidic condition (FA alone), N for neutral condition (FA/SA) and B for base condition (FA/KOH), left three are Co-N-C (NPs).

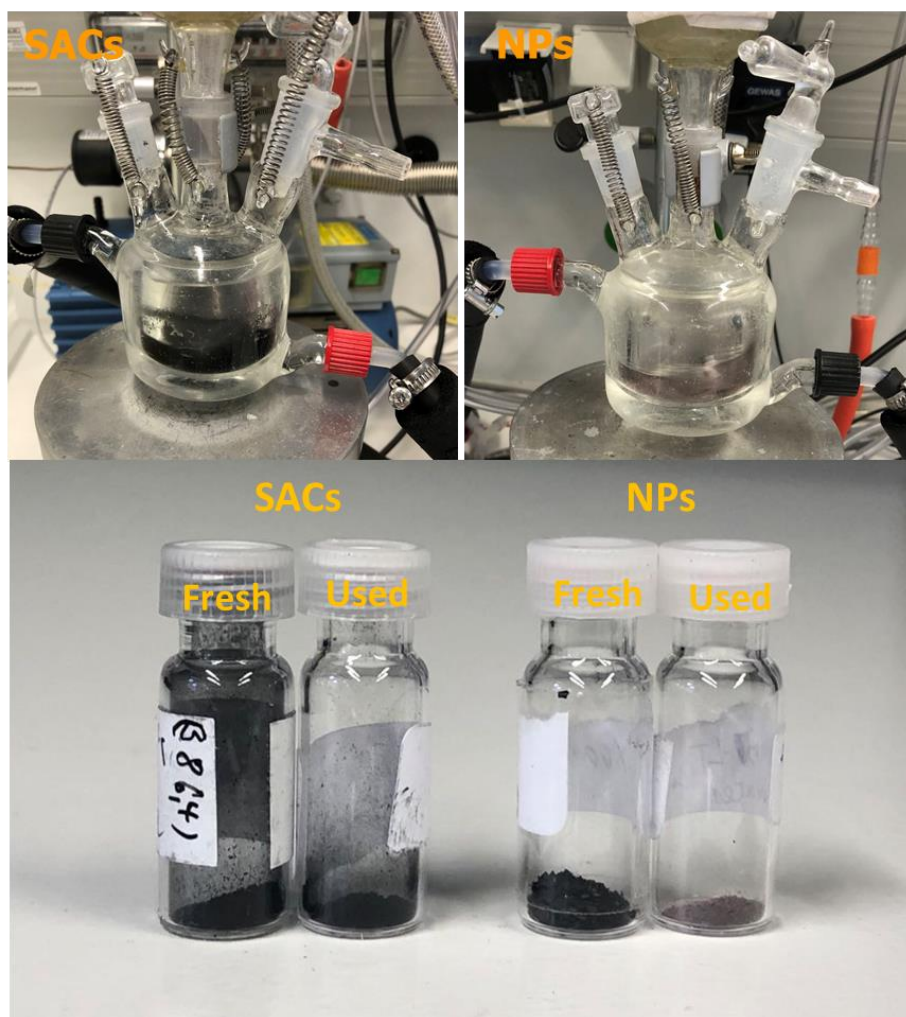


Figure S9. Phenomenon after reaction (water as solvent).



Figure S10. Phenomenon after reaction (PC as solvent).

Table S6. Co and N loss results after reaction by AAS

Catalyst	Solvent	Reaction time (min)	Color change	Co loss(%)	N loss(%)
Co-N-C (SACs)	PC	240	No	10.8	0.6
Co-N-C (NPs)	PC	240	No	38.1	41.5
Co-SACs	PC	7200	No	37	23.2
Co-NPs	PC	7200	No	49	61.1

8. Long-term Experiments

The reaction vessel was evacuated and refilled with argon for 6-8 times, FA (35 mmol, 1.32 mL) and PC (21 mL) were added to the vessel under argon flow, the thermostat was heated to the 110 °C (actual temperature 98 °C) and let equilibrate for 20 min. Then, the cobalt catalyst (30 mg) was added in a teflon crucible to the reaction vessel, setting this point as the starting point for measuring the evolved gas volume using a manual burette. The reaction was kept running for 120 h.

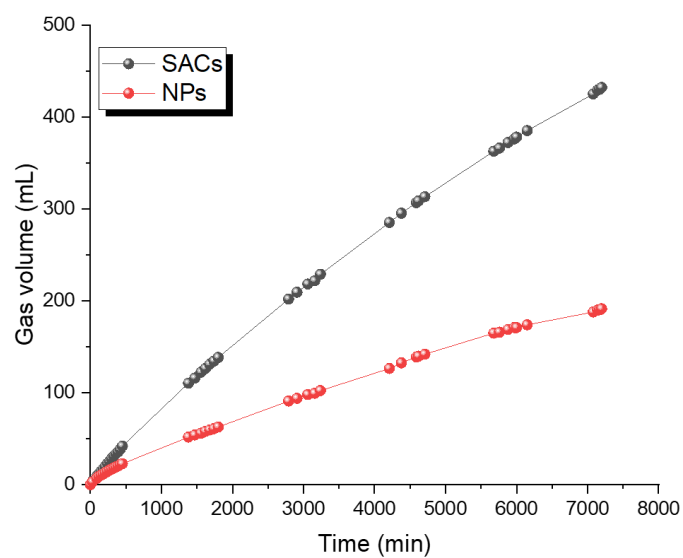


Figure S11. Long-term experiments.

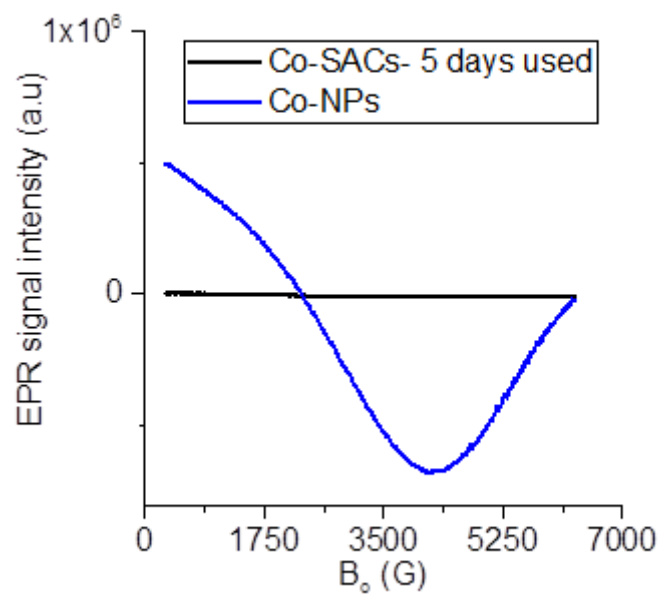


Figure S12. EPR spectra of Co-N-C(NPs) and Co-N-C(SACs) (after 7200h) measured at 100 K.

9. Fitting Results of EXAFS

Table S7. EXAFS fitting parameters at the Co K-edge for various samples ($S_0^2=0.73$)

Sample	Shell	N^a	$R(\text{\AA})^b$	$\sigma^2 \times 10^3(\text{\AA}^2)^c$	$\Delta E_0(\text{eV})^d$	R factor
Co foil	Co-Co	12*	2.49±0.01	6.4±0.1	8.2±0.2	0.001
Co ₃ O ₄	Co-O	4.3±0.4	1.92±0.01	3.0±0.3	-5.0±1.1	0.004
	Co-Co	2.7±0.5	2.85±0.01	2.0±0.9	-8.3±1.8	
	Co-Co	8.8±1.7	3.34±0.01	7.5±1.3	-9.7±1.6	
CoPc	Co-N	4.1±0.8	1.91±0.01	2.7±1.7	8.6±3.5	0.015
	Co-C	5.4±2.4	3.00±0.02	4.8±2.7	9.4±2.2	
Co samp	Co-N(O)	6.0±0.9	1.90±0.01	9.5±1.6	-6.7±2.0	0.011

^a N : coordination numbers; ^b R : bond distance; ^c σ^2 : Debye-Waller factors; ^d ΔE_0 : the inner potential correction. R factor: goodness of fit.

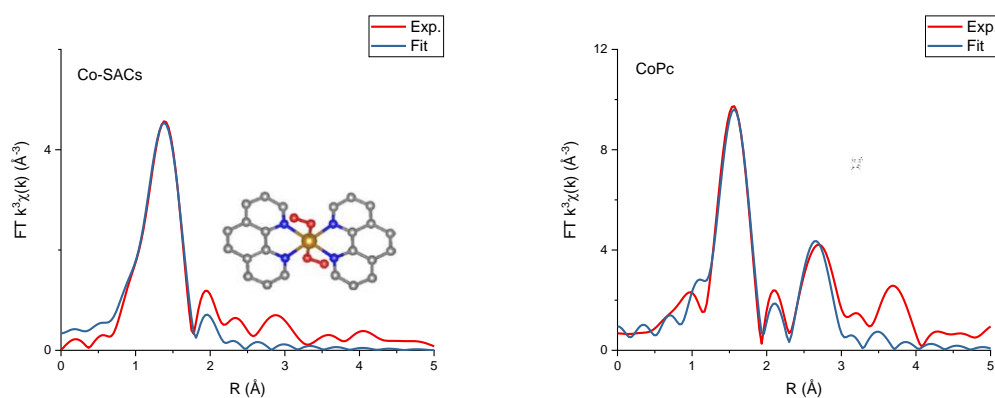


Figure S13. Fitting EXAFs spectrum of Co-N-C(SACs) and CoPc.

10. TEM

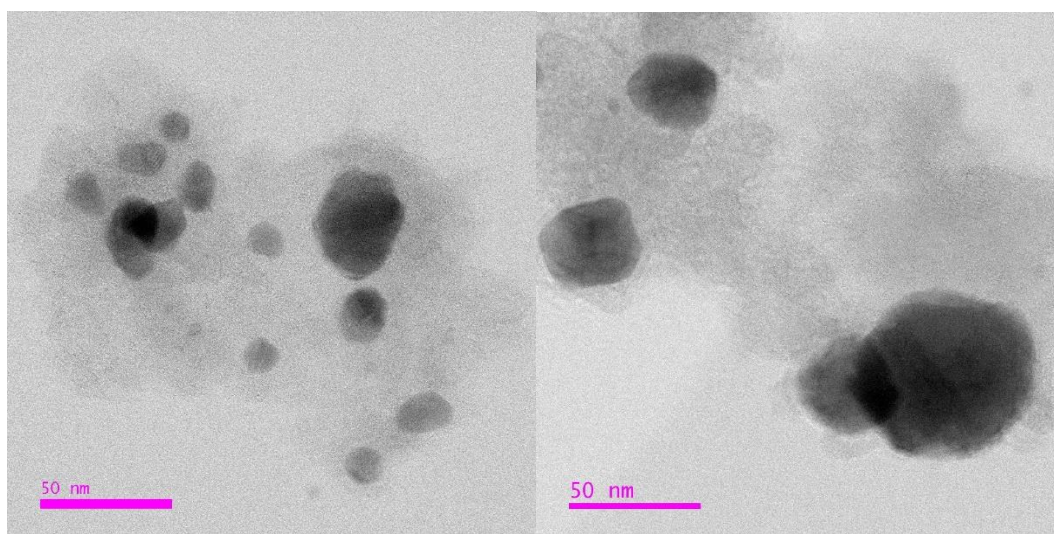


Figure S14. HRTEM images of Co-N-C(NPs)-900 (left) and Co-N-C(NPs)-1000 (right).

11.NMR

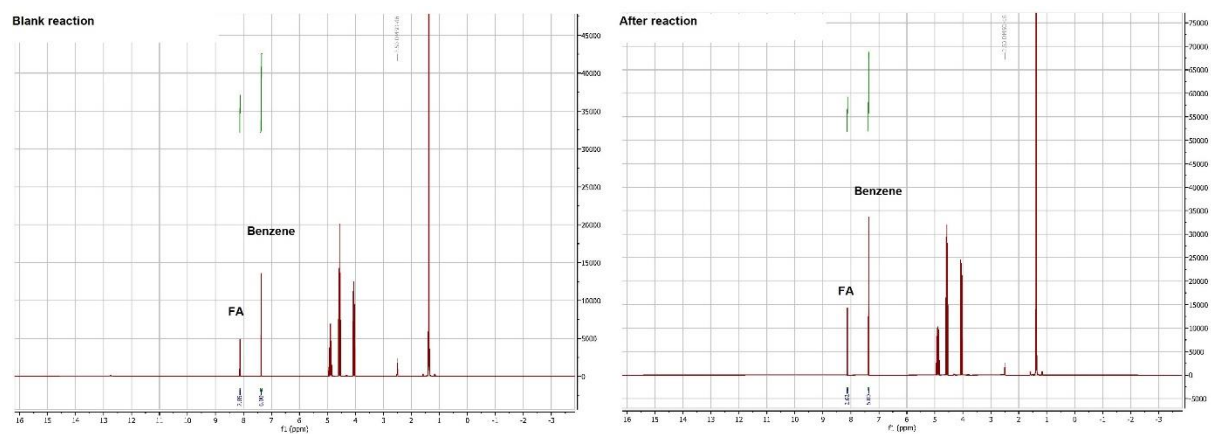


Figure S15. The NMR curves of blank (left) and end of reaction (right) with benzene as an inner standard.

12. Mechanistic Proposal for Formic Acid Dehydrogenation

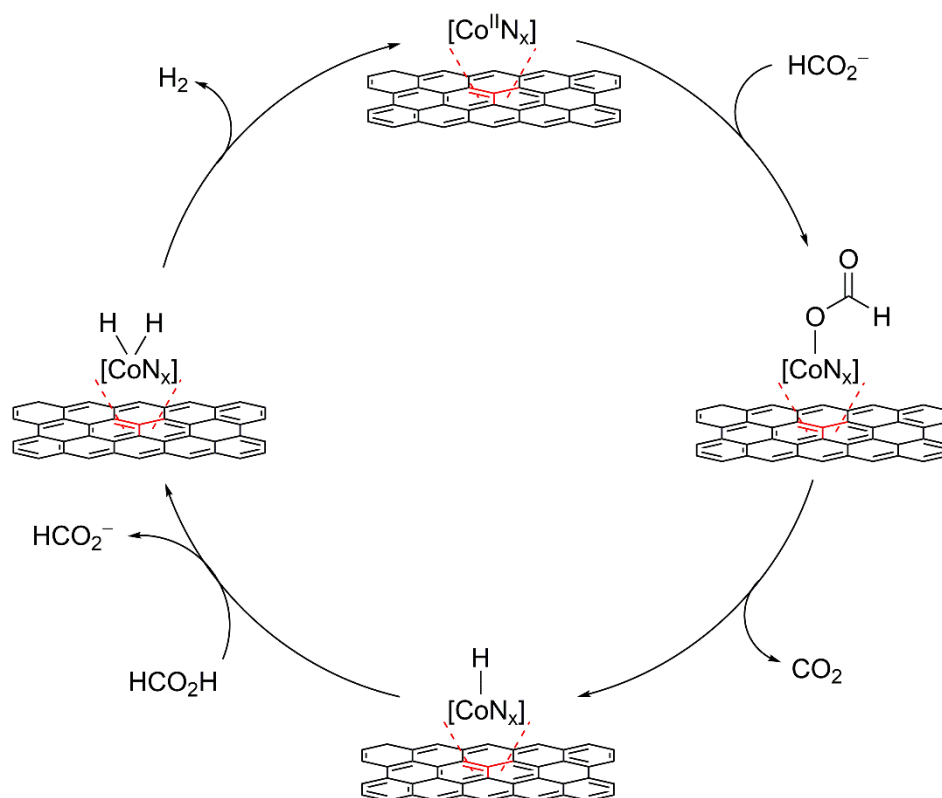


Figure S16. A general mechanistic proposal for formic acid dehydrogenation by Co-N-C(SACs) catalysts.

References

- [1] Z.-L. Wang, J.-M. Yan, H.-L. Wang, Y. Ping, Q. Jiang, *Sci. Rep.* **2012**, 2, 598.
- [2] D. A. Bulushev, M. Zacharska, E. V. Shlyakhova, A. L. Chuvilin, Y. Guo, S. Beloshapkin, A. V. Okotrub, L. G. Bulusheva, *ACS Catal.* **2016**, 6, 681.
- [3] M. Martis, K. Mori, K. Fujiwara, W.-S. Ahn, H. Yamashita, *J. Phys. Chem. C* **2013**, 117, 22805.
- [4] Ojeda, M.; Iglesia, E. *Angew. Chem., Int. Ed.* **2009**, 48, 4800.
- [5] Q. Y. Bi, X. L. Du, Y. M. Liu, Y. Cao, H. Y. He, K. N. Fan, *J. Am. Chem. Soc.* **2012**, 134, 8926.
- [6] Q. L. Zhu, N. Tsumori, Q. Xu, *J. Am. Chem. Soc.* **2015**, 137, 11743.
- [7] Q. Wang, N. Tsumori, M. Kitta, Q. Xu, *ACS Catal.* **2018**, 8, 12041.
- [8] S. Zhang, O. Metin, D. Su, S. Sun, *Angew. Chem., Int. Ed.* **2013**, 52, 3681.
- [9] O. Metin, X. Sun, S. Sun, *Nanoscale* **2013**, 5, 910.
- [10] H. Dai, N. Cao, L. Yang, J. Su, W. Luo, G. Cheng, *J. Mater. Chem. A* **2014**, 2, 11060.
- [11] X. Zhou, Y. Huang, W. Xing, C. Liu, J. Liao, T. Lu, *Chem. Commun.* **2008**, 3540.
- [12] H. M. Dai, B. Q. Xia, L. Wen, C. Du, J. Su, W. Luo, G.-Z. Cheng, *Appl. Catal. B* **2015**, 165, 57.
- [13] S. J. Li, Y. T. Zhou, X. Kang, D. X. Liu, L. Gu, Q. H. Zhang, J. M. Yan, Q. Jiang, *Adv. Mater.* **2019**, 31, 1806781.
- [14] M. Yurderi, A. Bulut, M. Zahmakiran, M. Kaya, *Appl. Catal. B: Environ* **2014**, 160–161, 514.
- [15] J. Cheng, X. Gu, P. Liu, T. Wang, H. Su, *J. Mater. Chem. A* **2016**, 4, 16645.
- [16] X. Zhou, Y. Huang, C. Liu, J. Liao, T. Lu, W. Xing, *ChemSusChem* **2010**, 3, 1379.
- [17] Z. L. Wang, J. M. Yan, Y. Ping, H. L. Wang, W. T. Zheng, Q. Jiang, *Angew. Chem., Int. Ed.* **2013**, 52, 4406.
- [18] Z. L. Wang, H. L. Wang, J. M. Yan, Y. Ping, S. I. O, S. J. Li, Q. Jiang, *Chem. Commun.* **2014**, 50, 2732.
- [19] Z. L. Wang, Y. Ping, J. M. Yan, H. L. Wang, Q. Jiang, *Int. J. Hydrogen Energy* **2014**, 39, 4850.
- [20] C. Tang, A. E. Surkus, F. Chen, M. M. Pohl, G. Agostini, M. Schneider, H. Junge, M. Beller, *Angew. Chem. Int. Ed.* **2017**, 56, 16616.